SUPPLEMENTARY MATERIALS

A shift in the ocean circulation has warmed the subpolar North Atlantic Ocean since 2016

Desbruyères et al. (2021)

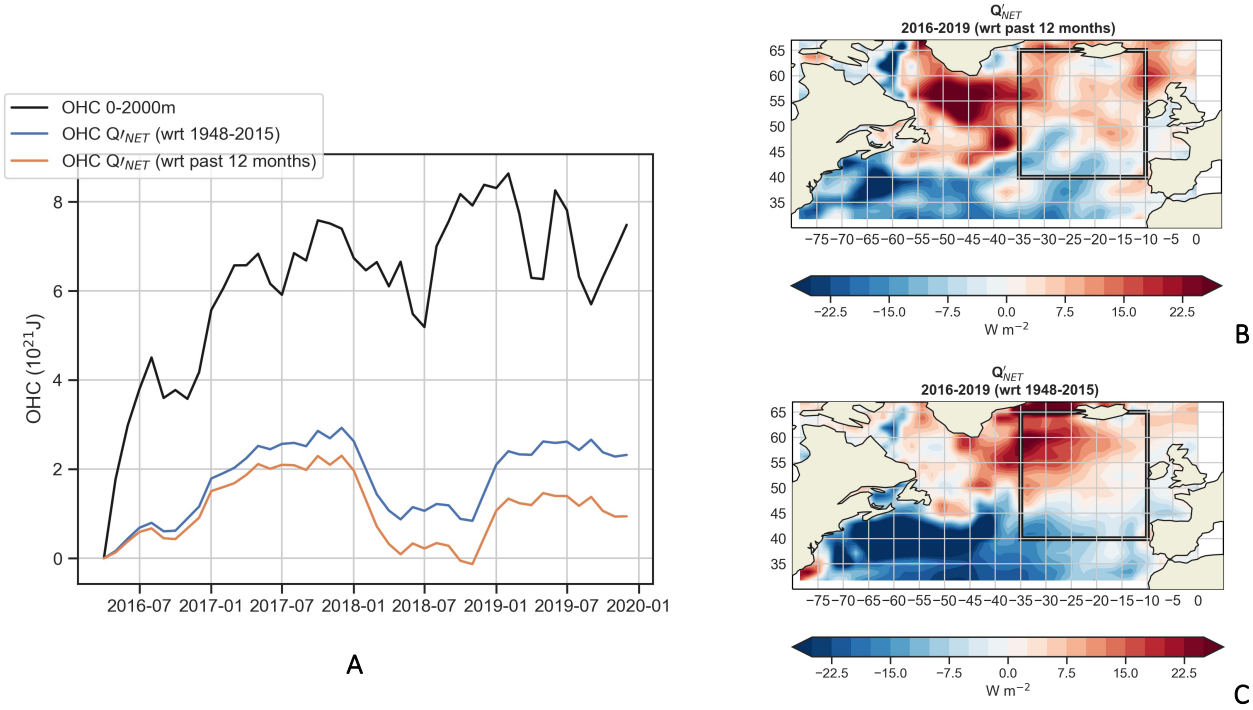

Supplementary Figure 1. 2016-2019 OHC changes driven by air-sea heat fluxes. (A) The estimated contribution of anomalous NCEP air-sea heat fluxes Q_{NET} to the observed 0-2000 m ocean heat content changes (OHC) in the eastern SPNA (black line; see black box in (B)) since April 2016 (i.e. the onset of the trend reversal). Because Q_{NET} anomalies (and their subsequent temporal accumulation) depend on the subjective choice of a reference period, two distinct cases are here shown in which anomalies are obtained from (1) the long-term climatology 1948-2015 (blue) and (2) the average of the 12 months preceding the warming onset (orange). Q_{NET} was initially detrended. (B) and (C) The distribution of Q_{NET} anomalies as averaged during April 2016 – December 2019 with respect to the two reference periods.

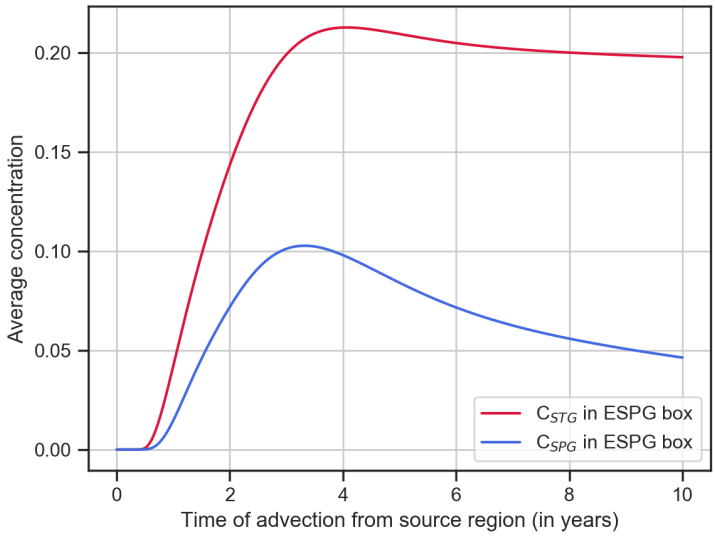

Supplementary Figure 2. Validation of forward advective timescales. The mean concentration of tracers in the eastern SPNA box as a function of advection time from the western SPG (blue) and western STG (red) boxes (see Figure 3 for boxes locations), as obtained from 10 years of forwards advection within the time-mean (2002-2019) altimetry-derived surface geostrophic velocity field. The tracer concentration was averaged at each time step within the eastern SPNA box, providing a quantification of a typical time of advection from both regions. The peak in the distributions indicates the time from which more tracers are leaving the eastern SPNA box than entering it. Since we are interested in circulation changes that affect the upstream inflow of cold SPG waters and warm STG waters and eventually their relative proportion within the eastern SPNA, advective time scale smaller than the peak in the distribution (N = 2, 3 and 4 years) are used in the analysis of interannual-decadal variability (i.e. we only consider the time-span during which subtropical and subpolar tracers are predominantly building up within the ESPG). This choice is in line with the literature-based estimation of the advective timescales from between the two source regions and the eastern SPNA[28,29]

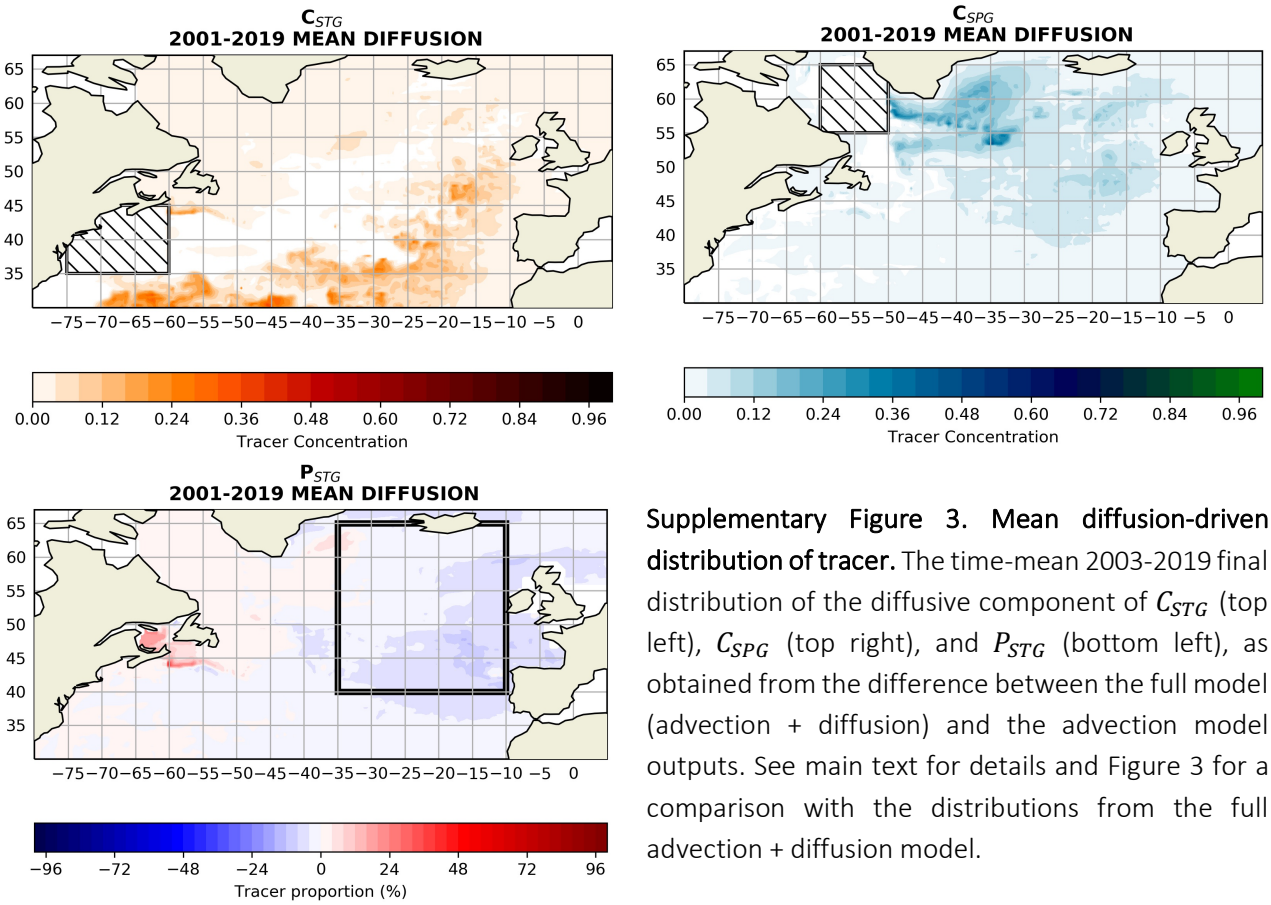

Supplementary Figure 3. Mean diffusion-driven distribution of tracer. The time-mean 2003-2019 final distribution of the diffusive component of C_{STG} (top left), C_{SPG} (top right), and P_{STG} (bottom left), as obtained from the difference between the full model (advection + diffusion) and the advection model outputs. See main text for details and Figure 3 for a comparison with the distributions from the full advection + diffusion model.

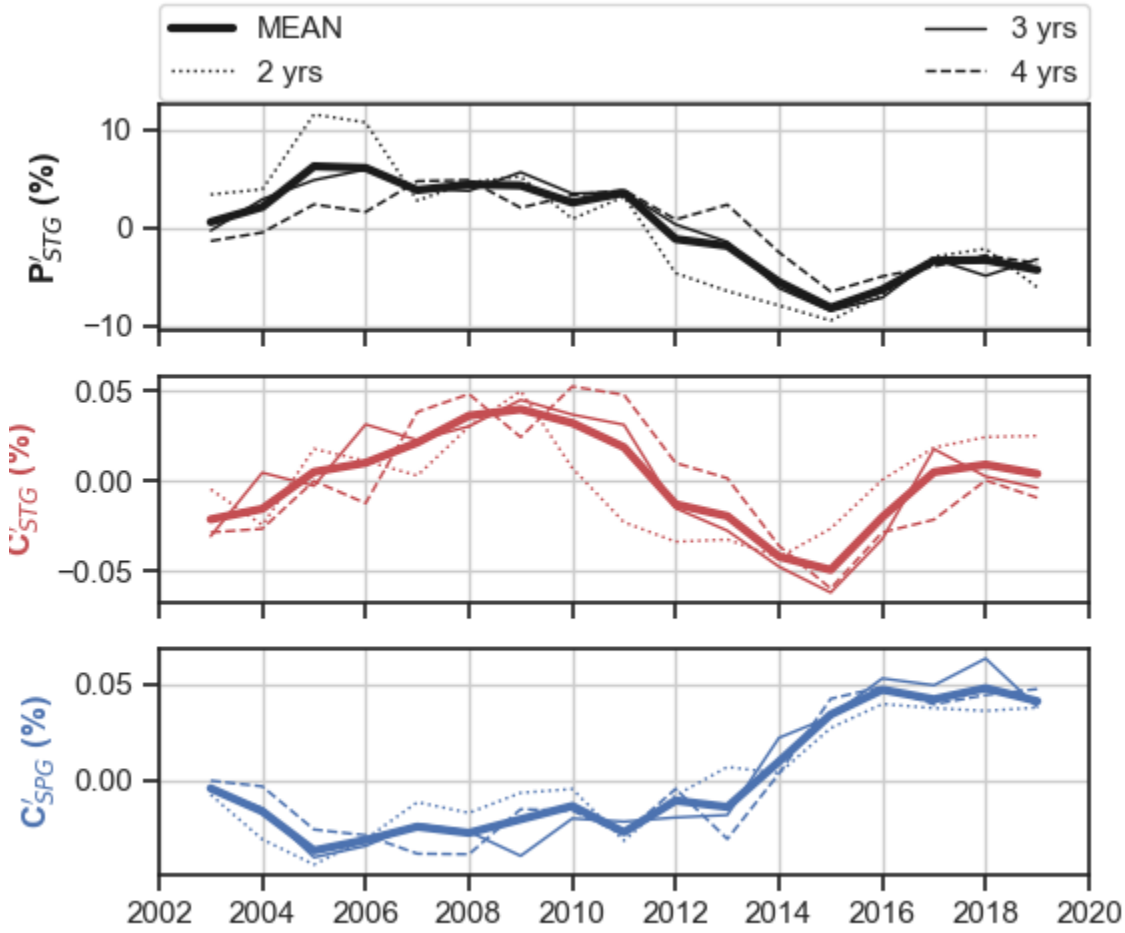

Supplementary Figure 4. Sensitivity to advective timescales. P'_{STG} (black), C'_{STG} (red) and C'_{SPG} (blue) for three different integration times of equation 1: $N = 2$ years (dotted), $N = 3$ years (solid), and $N = 4$ years (dashed). The mean (thick solid lines) time series are the ones shown in Figure 4. We here demonstrate the robustness of the methods and its small sensitivity of the results to the choice of typical surface advective timescales.

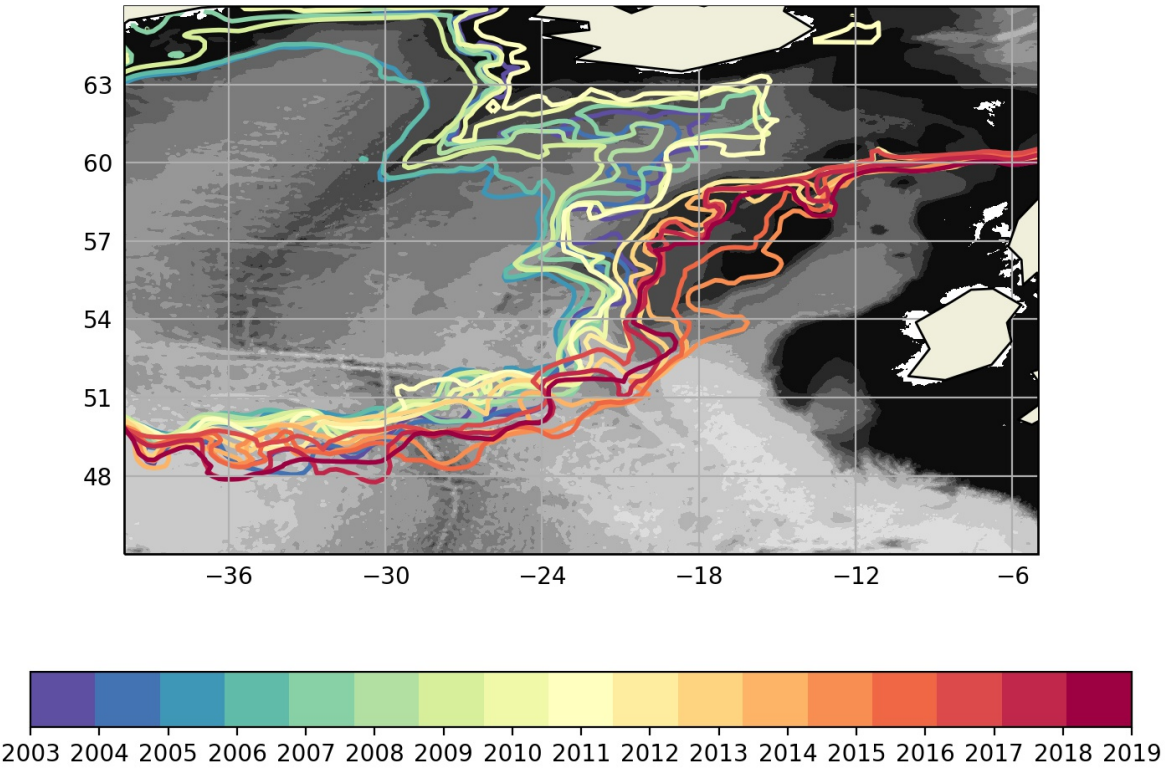

Supplementary Figure 5. Subpolar front displacements. The yearly position of the 50% P_{STG} isoline. The latter is an estimate of the subpolar front, whose movements are often referred to as "contraction" and "expansion" of the SPG. Here, it started moving northwestward since 2016 following the recent cooling-to-warming reversal, reaching a position in 2019 similar to that observed in 2012.

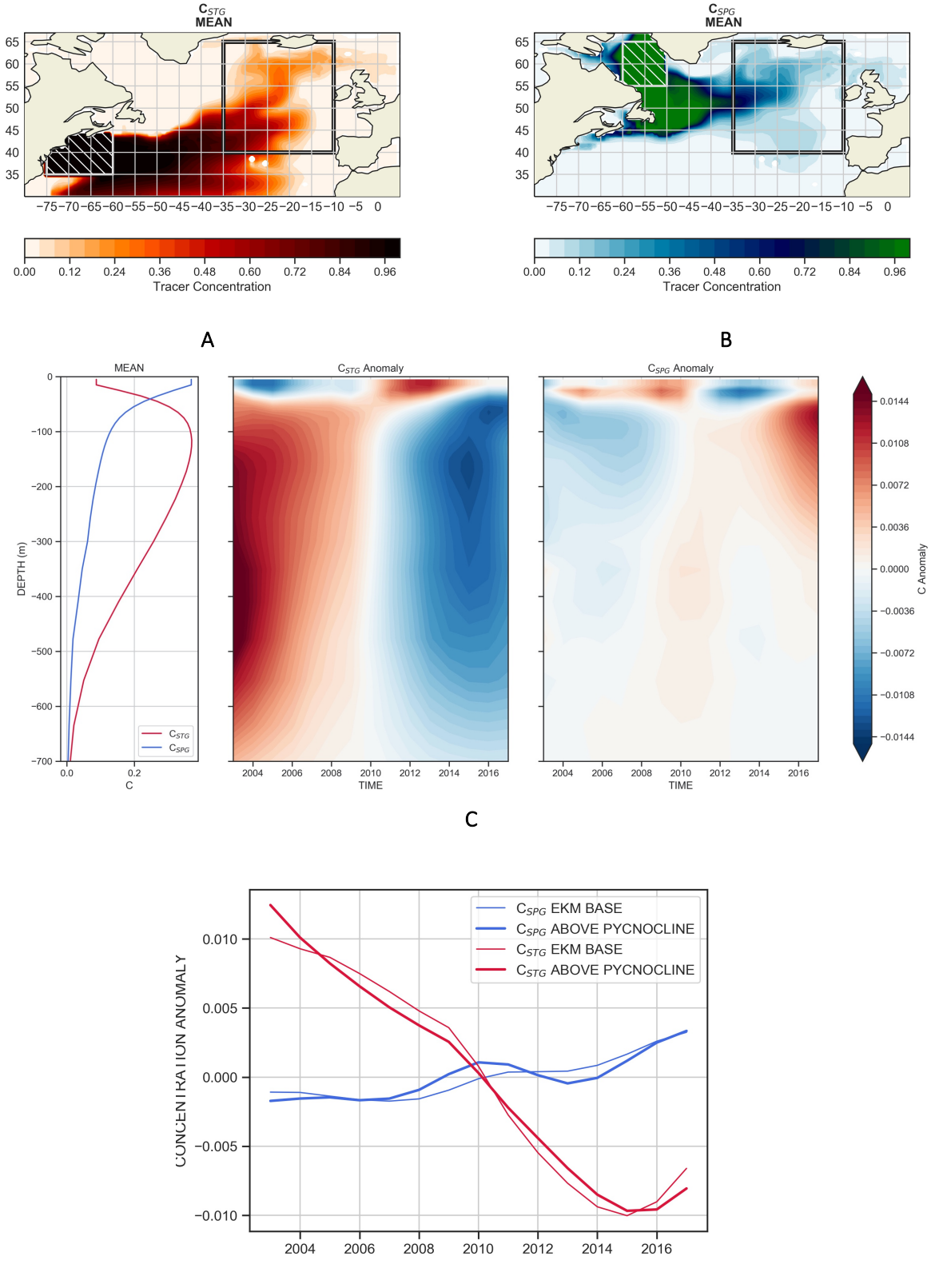

Supplementary Figure 6. Tracer advection in ECCOv4r4 velocity field. (Top) The time-mean 2003-2017 final distribution of C_{STG} and C_{SPG} above the main pycnocline (σ_0 = 27.6) following N years of tracer advection within the 3D velocity field of the ECCOv4r4 ocean reanalysis (the ensemble mean of N = 2, 3 and 4 years is

shown). Tracer are kept to unity within the full water column of the source regions and advected freely forward in time in a model setup identical to that used in the altimetry-based experiment but augmented by a vertical component of advection (see text and Methods). (Bottom) The mean and anomalous vertical distribution of C_{STG} and C_{SPG} above the main pycnocline and averaged within the eastern SPNA (black box).). (D) The (normalized) concentration anomalies of C_{STG} and C_{SPG} in the eastern SPNA at 100m (base of the Ekman layer, thin lines) and as averaged above the main pycnocline (thick lines).

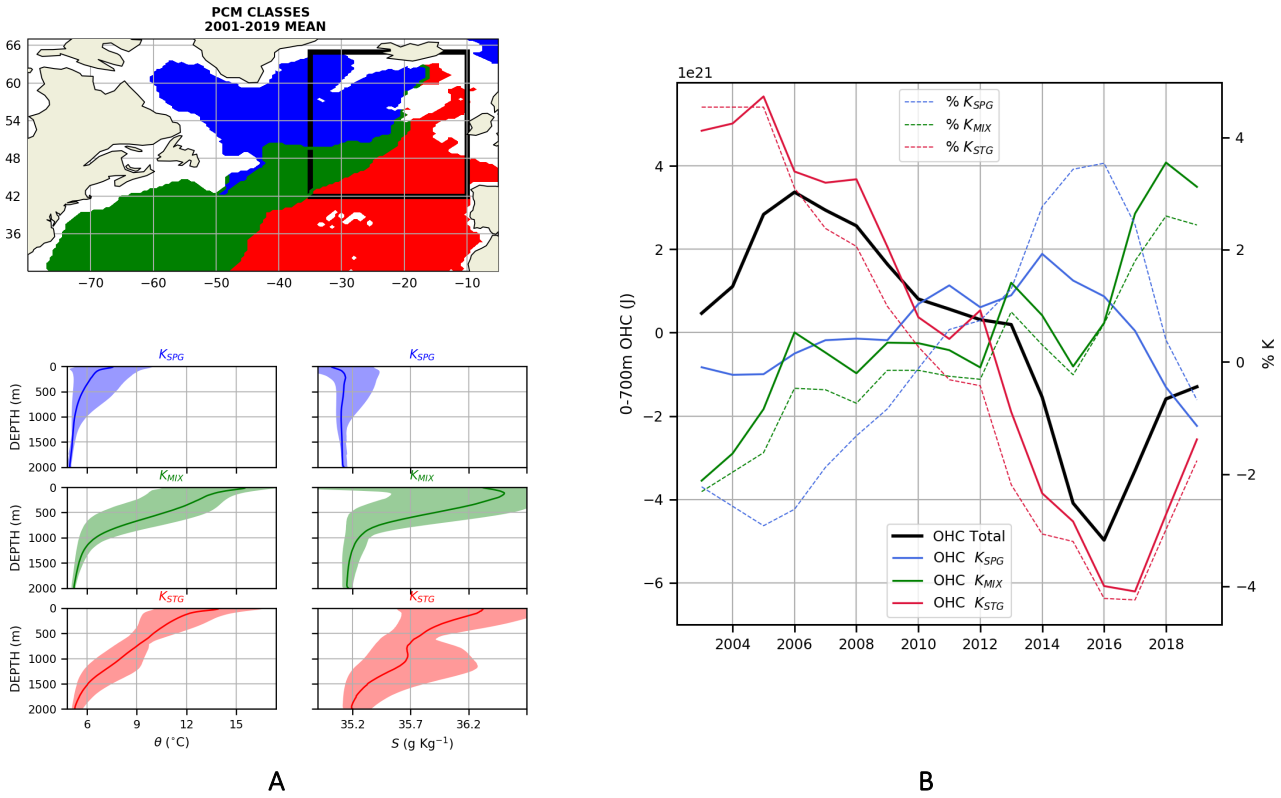

Supplementary Figure 7. PCM with 3K. (A) The horizontal distribution of the three classes K_{STG} (red), K_{SPG} (blue) and K_{MIX} (green) obtained from the long-term mean (2003-2019) temperature and salinity fields, along with their respective temperature and salinity vertical structures. (B) The OHC of the upper 0-700m layer of the eastern SPNA (black box, black line) decomposed into contributions from K_{SPG} (solid blue), K_{STG} (solid red) and K_{MIX} (solid green). Anomalies in the proportion of those three classes are shown with dashed lines. The additional cluster from the K=2 case presented in the paper (Figure 5) is primarily splitting the western and eastern structure of the subtropical gyre, i.e. clusters green and red with K=3 are mostly made of cluster red with K=2. This highlights the role played by the salty Mediterranean Waters in affecting the interior salinity structure of the North Atlantic.

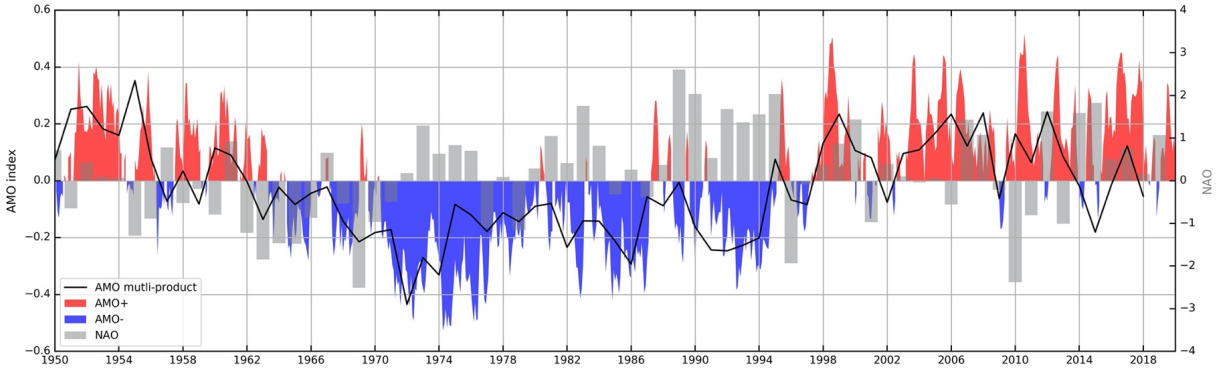

Supplementary Figure 8. Atlantic Multidecadal Oscillation (AMO)and North Atlantic Oscillation (NAO). The red/blue shading shows the monthly AMO index of [39] between 1950 and May 2020. The black line shows an AMO index as an ensemble mean of four different indices calculated based on two different definitions (see[41]). Gray bars show a normalized winter index of the North Atlantic Oscillation (NAO)[54].

60